Compressible turbulent flows: modeling and similarity considerations

By O. Zeman

1. Motivations and objectives

With the recent revitalization of high speed flow research, compressibility presents a new set of challenging problems to turbulence researchers. Questions arise as to what extent compressibility affects turbulence dynamics, structures, the Reynolds stress-mean velocity (constitutive) relation, and the accompanying processes of heat transfer and mixing. In astrophysical applications, compressible turbulence is believed to play an important role in intergalactic gas cloud dynamics and in accretion disk convection.

Our work is principally directed toward understanding and modeling of the compressibility effects in free shear flows, boundary layers, and boundary layer/shock interactions.

2. Introduction

Compressibility effects in turbulent flows depend mainly on the r.m.s. fluctuating Mach number M_t, defined as the ratio of the r.m.s. fluctuating velocity to the mean field sonic velocity. Direct numerical simulations (DNS) of homogeneous turbulence indicate that when $M_t \leq 0.1$, the turbulence dynamics is generally unaffected by compressibility. It means that the vortical (solenoidal) and the compressive (acoustic) modes of the fluctuating field are virtually decoupled (Kovásznay, 1953). Only when M_t exceeds a value of about 0.3 does compressibility begin to noticeably influence turbulence dynamics and structure. Further increase in M_t may lead to the formation of shock-like structures, or turbulent shocklets. Shocklet formation has been recently detected in the DNS of decaying turbulence by Lee, Lele, and Moin (1990). In the DNS of homogeneous shear turbulence, Blaisdell (1990) detected the shocklets for $M_t \geq 0.7$. Zeman (1990) suggested that weak shocklets may be responsible for the growth rate attenuation in shear layers and proposed a physical model for shocklet formation and the associated (dilatation) dissipation. On the basis of the DNS results and experimental evidence in mixing layers (e.g. Papamoschou and Roshko 1988), compressibility effects may be broadly classified by the magnitude of M_t. Thus we shall refer to the range $0.3 < M_t < 0.6$ as moderate Mach numbers whereby the compressibility effects are observable but with shock-like occurrences being statistically insignificant. At large Mach numbers $M_t > 0.6$, a full scope of compressibility-induced effects may be expected, such as shocklet and baroclinic vorticity generation and significant solenoidal/compressive mode interactions.

3. Accomplishments

The accomplishments described in the following subsections consist of: The study of similarity in supersonic mixing layers (2.1), description of the new proposed

model for the pressure-dilatation term and its application in decaying turbulence (2.2), the study of constitutive relations in compressible shear-driven turbulence (2.3), and current work concerning the effect of mean compression on turbulence as in the turbulence/shock interactions (2.4).

3.1. Similarity in supersonic mixing layers

The most prominent effect of compressibility on mixing layers is inhibition of the layer growth as observed in experiments e.g. by Bogdanoff (1983), Papamoschou and Roshko (1988), and Samimy and Elliott (1990) among others. These findings have been unified by the concept of the so-called convective Mach number (M_c) introduced by Bogdanoff and Papamoschou & Roshko, wherein properly normalized growth rates are expected to be solely a function of M_c. The experimental data suggest that the growth rate decreases appreciably for convective Mach numbers in the range between 0.3 and 1.2; beyond $M_c = 1.5$ the growth rates level off at about 30% of the low speed value.

Zeman (1990a) (hereafter referred to as Z90) suggested that growth inhibition in mixing layers is related to dilatation dissipation, ϵ_d. Dilatation dissipation occurs in regions where fluid elements acquire supersonic relative speeds and form shock-like structures called shocklets. These structures generate high levels of ϵ_d. In mixing layers, the shocklet contribution to dilatation dissipation is expected to become important when the Mach number M (based on the relative velocity difference $\triangle U = U_1 - U_2$ of the free streams) is about one (or $M_c \approx 0.5$). This value appears to coincide with the onset of growth rate reduction.

There is so far no satisfactory physical explanation for the leveling of the growth rates at large convective Mach numbers ($M_c > 1.2$). As shown in Z90, a second-order closure model which accounts for shocklet dissipation predicts this leveling reasonably well, and one could argue that for larger Mach numbers (say $M_c > 1.5$), the velocity fluctuations are controlled (through the shocklet dissipation) by the local sonic velocity and not by the velocity difference $\triangle U$. Evidence of this effect is shown in Fig. 5 of Z90, where the modeled r.m.s. Mach number at the mixing layer centerline is plotted vs. $M = 2M_c$. As M increases beyond a value of 3, M_t approaches an asymptotic (saturation) limit $M_t \rightarrow M_{t\infty} \approx 0.5$, suggesting that r.m.s. turbulent fluctuations are determined by the local sonic speed, $q \propto a(T)$. This result forms the starting point and basis for a similarity theory for supersonic mixing layers. The theory has been described in Zeman (1990b), and the following is its brief summary.

3.1.1 Outline of the similarity theory

In shear layers of practical interest, the turbulent Reynolds number $R_e = u'\ell/\nu$ is sufficiently large so that terms of order $O(R_e^{-1})$ or smaller can be neglected (here, u', ℓ are, respectively, the turbulence velocity and length scales). Furthermore, because the value of the layer growth rate $d\delta/dx$ is a small number (for $M_c > 1$, $d\delta/dx < 0.03$), it is permissible to invoke the thin-layer approximation and the Favre-averaged equations for mean density, velocity, enthalpy, and pressure

(ρ, U_i H, P), then reduce to

$$\frac{\partial \overline{\rho}\widetilde{U}_j}{\partial x_j} = 0 \tag{1}$$

$$\overline{\rho}\widetilde{U}_j \frac{\partial \widetilde{U}_1}{\partial x_j} = -\frac{\partial \overline{\rho}\widetilde{u_1 u_2}}{\partial x_2} \tag{2}$$

$$c_p \overline{\rho}\widetilde{U}_j \frac{\partial \widetilde{T}}{\partial x_j} = -\frac{\partial \overline{\rho}\widetilde{hu_2}}{\partial x_2}\frac{1}{\gamma} + \rho\epsilon_{tot} - \overline{pu_{j,j}} \tag{3}$$

$$\overline{\rho} = \frac{p_o}{RT + \overline{u_2^2}} \tag{4}$$

The axes $x_1 \equiv x$, $x_2 \equiv y$ are oriented in the streamwise and transverse directions respectively; the factor $1/\gamma$ in (3) stems from absorption of the pressure flux $\overline{pu_2}$ into the enthalpy flux. As shown in Z90, ϵ_{tot} consists of solenoidal and dilatation contributions and can be expressed as $\epsilon_{tot} = \epsilon_s(1 + F(M_t))$. For the purpose of similarity analysis, it is more convenient to deal with energy production; in the turbulence energy budget of mixing layers about 90 percent of the turbulence (shear) production is dissipated; we make a convenient approximation $\rho\epsilon_{tot} - pu_{j,j} \approx -\overline{\rho}\widetilde{u_1 u_2}\widetilde{U}_{1,2}$. Seeking the similarity solutions to (1)-(4), we assume possible similarity functions for mean velocity and temperature as follows

$$\widetilde{U}(x,y) = U_c + \triangle U f(\eta) \tag{6}$$

$$\widetilde{T}(x,y) = T_o + \triangle T \theta(\eta) \tag{7}$$

The subscript 'c' designates variables at the mixing layer centerline $y = y_c$; $\eta = (x - y_c)/\delta_\omega$ is the similarity variable where $\delta_\omega = \triangle U/(\partial U/\partial y)_c$, and $\triangle T = T_c - T_o$ is the temperature excess. The appropriate boundary values are $f = 0$, $\theta = 1$ at $\eta = 0$, and $f = 1/2$, $\theta = 0$ at $\eta = \infty$.

Similarity solutions exist only if the differential equations for functions $f(\eta)$ and $\theta(\eta)$ are independent of the parameters of the flow, the Mach number $M = \triangle U/a_o = 2M_c$, and the ratio $\triangle U/U_c$. By scaling argument, it can be inferred from (4)-(8) that

$$\triangle T/T_o = \alpha M^2, \tag{8}$$

where the empirical constant α has been determined from the modeling results as $\alpha \approx 0.05$ (Zeman, 1990a). Finally, assuming that the concept of eddy viscosity (K) and diffusivity (K_h) remains valid in compressible regime, we obtain

$$-\frac{\delta'_\omega U_c}{\triangle U} f' \int_0^\eta \overline{\rho}(1 + \frac{\triangle U}{U_c} f) d\eta = \frac{K_c}{\triangle U \delta_\omega}(\frac{K}{K_c}\overline{\rho} f')', \tag{9}$$

and

$$-\frac{\delta'_\omega U_c}{\triangle U}\theta' \int_0^\eta \overline{\rho}(1 + \frac{\triangle U}{U_c} f) d\eta = \frac{K_c}{\triangle U \delta_\omega}[(\gamma P_{rt})^{-1}(\frac{K}{K_c}\overline{\rho}\theta')' + \beta\overline{\rho}\frac{K}{K_c}(f')^2]. \tag{10}$$

The constant $\beta = \alpha^{-1}R/c_p$ is associated with the heating term in the energy equation (10); this term is responsible for the density variation and coupling of the energy and momentum equations. In view of the similarity analysis, it is important to note that: i) according to the experimental evidence, the growth rate parameter $\delta'_\omega U_c/\Delta U$ appearing in (9) and (10) is dependent on M; ii) the turbulence Reynolds number $R_T = \Delta U \delta_\omega / K_c$ is also a function of M, since by definition

$$R_T^{-1} = \frac{K_c}{\Delta U \delta_\omega} = \frac{u_*^2}{\Delta U^2}, \tag{11}$$

where u_*^2 designates the centerline Reynolds shear stress $-\widetilde{uv}_c$. The ratio $u_*/\Delta U$ decreases with M as shown experimentally by Samimy and Elliott (1990). Without loss of generality, we shall assume that $\Delta U/U_c << 1$ so that this parameter may be eliminated from similarity consideration.

The density $\overline{\rho}/\rho_o = (1+\alpha M^2\theta(\eta))^{-1}$ cannot be expressed as a similarity function and, therefore, in principle the proposed similarity functions $f(\eta)$, $\theta(\eta)$ do not exist unless $M \to \infty$. However, an approximate similarity will always be possible near the core of the layer where $\theta(\eta) \approx 1$. Then, the standard similarity requirements to be satisfied are

1) Eddy viscosity profiles in (9), (10) be selfsimilar, i.e. $K/K_c = \kappa(\eta)$ and
2) The coefficients in the differential equations (9), (10) be proportional, i.e.

$$C_\delta \equiv \frac{\delta'_\omega U_c}{\Delta U} \propto \frac{1}{R_T} = \frac{u_*^2}{\Delta U^2}, \tag{13}$$

Now, as mentioned earlier, the (centerline) r.m.s. Mach number approaches for $M \geq 3$ a saturation limit $M_{t\infty}$, and all Reynolds stress components must be proportional to the square of the sonic speed a_c; i.e., $\widetilde{u_i u_j}_c \propto u_*^2 \propto a_c^2$ where $a_c = a_o\sqrt{1+\alpha M^2}$. Then, according to (13), we obtain the principal result of the similarity analysis—that the nondimensional growth rate C_δ is related to M through the relation

$$C_\delta \propto \frac{u_*^2}{\Delta U^2} \propto \frac{1+\alpha M^2}{M^2}. \tag{14}$$

A comparison between the parametric formula (14), experiments, and the Z90 model results are shown in Fig. 1. We remark that the experimental growth rates in Fig. 1 are inferred from a momentum or Pitot probe thickness; these, in general, differ from the growth rates based on the vorticity thickness δ_ω. The plots of functions $f(\eta)$, $\theta(\eta)$ (shown in Zeman, 1990b) indicate that both the computed mean temperature and velocity profiles converge to selfsimilar shape for $M \geq 3$. Zeman (1990b) has also shown that the normalized stresses follow the similarity law

$$\frac{\widetilde{u_i u_j}}{\Delta U^2} \propto \frac{1+\alpha M^2}{M^2} g_{ij}(\eta). \tag{15}$$

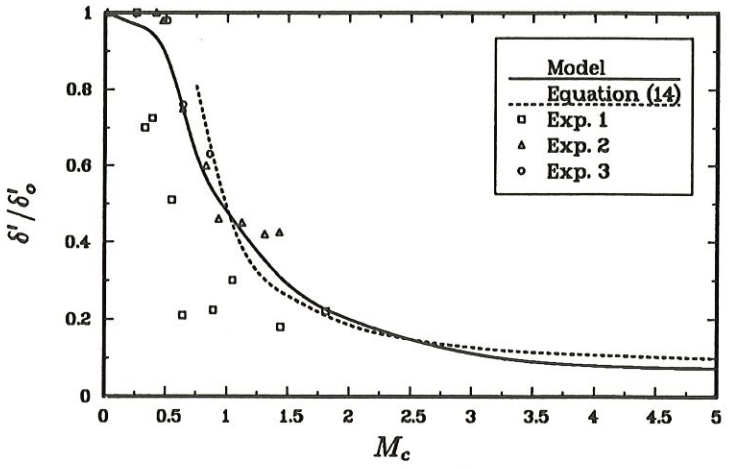

FIGURE 1. Normalized growth rate vs. $M_c = \frac{1}{2}M$. Exp. 1 and 2 denote data from Papamoschou and Roshko (1988), 3 are data of Samimy and Elliott (1990)

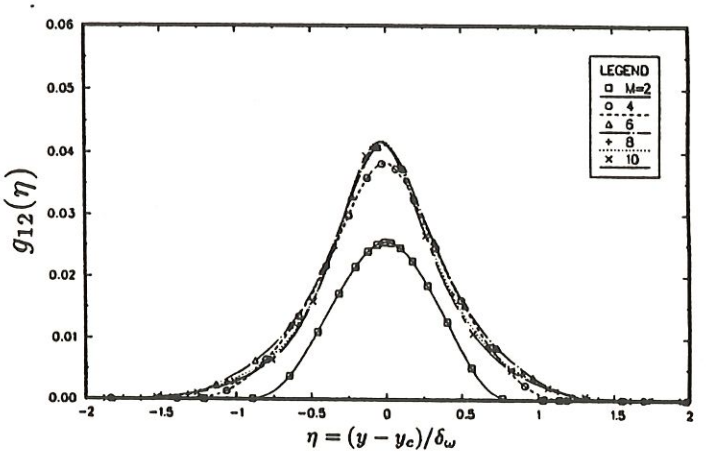

FIGURE 2. Shear stress similarity function $g_{12}(\eta) = -\frac{\widetilde{u_1 u_2}}{\Delta U^2}\frac{M^2}{1+\alpha M^2}$.

The function $g_{12}(\eta)$ corresponding to the shear stress $\widetilde{u_1 u_2}$ is shown in Fig. 2. The function g_{12} is seen to collapse to a self-similar form for $M \geq 4$.

In conclusion, it is evident that although the similarity requirements in compressible mixing layers are incomplete, the proposed similarity laws represented by equations (13)-(15) yield, for all practical purposes, useful estimates of expected temperatures and turbulence quantities in high Mach number shear layers.

3.2. Pressure-dilatation and compressible turbulence decay

It has been shown in Z90 that in the Reynolds stress equations for homogeneous turbulence, one can identify two principal compressible terms: the dilatation dissipation ϵ_d and the pressure-dilatation correlation $\overline{pu_{j,j}}$. In equilibrium mixing layers, the pressure-dilatation was estimated as negligible (Z90); however, in temporally

evolving flows, this is not so, and $\overline{pu_{j,j}}$ has to be considered. For convenience, we shall hereafter use the identity $\overline{pu_{j,j}} = \bar{\rho}\Pi_d$, where Π_d has the same dimension as ϵ_d (rate of energy per unit mass).

The following two findings were described in Zeman (1990c), and in Zeman and Blaisdell (1990). First, considering shockless turbulence, Zeman (1990c) inferred an approximation

$$\Pi_d \approx -\frac{1}{2}\frac{D\overline{p^2}}{Dt}\frac{1}{(\bar{\rho}a)^2}. \tag{16}$$

According to the Blaisdell DNS results, the above approximation is well satisfied at Mach numbers as high as $M_t = 0.7$ both in decaying and shear-driven turbulence (see Fig. 3). Equation (16) is exact in linear acoustics. Second, in order to close (16), Zeman (1990c) suggested that the pressure variance will tend to relax to its equilibrium value (p_e^2) on the time scale (τ_a) associated with the propagation speed of pressure perturbations,

$$\frac{D\overline{p^2}}{Dt} = -\frac{\overline{p^2} - p_e^2}{\tau_a}. \tag{17}$$

By means of scaling arguments, the equilibrium pressure has been related to q^2 and M_t by the parametric relation

$$\frac{p_e^2}{\bar{\rho}^2 q^2 a^2} = P_e(M_t) = \frac{\alpha M_t^2 + \beta M_t^4}{1 + \alpha M_t^2 + \beta M_t^4}. \tag{18}$$

Optimal values of the adjustable constants in (18) are $\alpha = 0.8$, $\beta = 1.0$. Chandrasekhar (1952) showed that the propagation speed of density (or pressure) perturbations in isotropic turbulence is $c = a\sqrt{2 + \frac{2}{3}M_t^2}$, which yields with certain approximations $\tau_a \approx 0.13\tau M_t$. The turbulence time scale is, as usual, related to the solenoidal field, which dominates the turbulence dynamics even in the compressible regime, i.e., $\tau = q^2/\epsilon_s$. Also, the model equation for the solenoidal dissipation $(D\epsilon_s/Dt \propto -\epsilon_s/\tau)$ remains independent of compressibility, i.e. of M_t.

A model-DNS comparison of the decay of compressible turbulence with initial $M_{to} = 0.7$ and $(\overline{p^2}/\bar{p}^2)_o = 0.045(\gamma M_{to})^2$, is displayed in Figs. 3 and 4 (see also Zeman and Blaisdell, 1990). Fig. 3 shows the evolution of the pressure dilatation term normalized by the initial (solenoidal) dissipation, Π_d/ϵ_{so}. The evolution time t is normalized by half the initial time scale $\tau_o = (q^2/\epsilon_s)_o$. Fig. 3 also displays the validation of (16): the dashed and dotted lines are, respectively, DNS computed data of the left-, and right-hand sides of (16). Fig. 4 presents a similar graph for the pressure variance normalized by mean pressure. Important properties of the present model are that

1) it is capable of predicting a correct magnitude of Π_d/ϵ_{so} which may vary, depending on initial conditions, by an order of 100 (see Zeman and Blaisdell, 1990);

2) as indicated in Fig. 4, the Π_d-model provides a correct amount of energy transfer to the fluctuating pressure field, including the time scale of the transfer. Overall, although the Π_d-model does not agree with the DNS data in every detail, its integral effect, which dictates the overall energy transfer, is physically correct. Another

example of compressible decay (given in Zeman and Blaisdell, 1990) involves initial conditions when $M_t < 0.1$ is very small but the pressure fluctuation content is high, i.e., $\overline{p^2}/\overline{p}^2 > (\gamma M_t)^2$. In that case, the initial energy transfer is reversed and the potential energy residing in the pressure field is converted into kinetic energy. This causes an initial rapid increase in q^2. Again, the present model is capable of capturing the basic physics of this process.

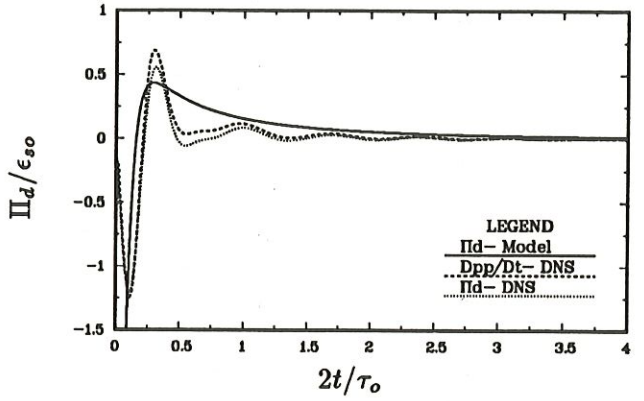

FIGURE 3. Model-DNS comparison: pressure-dilatation evolution.

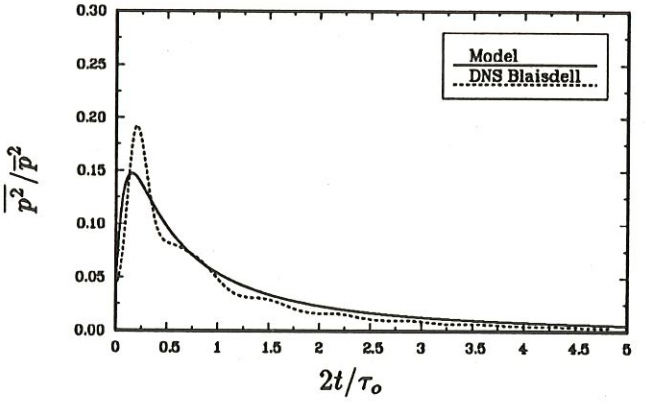

FIGURE 4. Model-DNS comparison: pressure variance evolution.

3.3. Compressible shear turbulence

To the first order approximation, the compressibility terms inferred for decaying turbulence are unaffected by the presence of mean shear, and the pressure-dilatation model outlined in the previous section remains the same for the homogeneous shear turbulence. Furthermore, on the basis of the differential equations for fluctuating pressure, one can argue that the slow and rapid pressure terms in the Favre-averaged setting will retain their incompressible forms so that the direct compressibility contributions in the Reynolds stress equations will be again the dilatation dissipation and pressure dilatation terms.

With the mean shear $dU_1/dx_2 = S$, the actual set of equations needed to compute the (Favre-averaged) stress components $R_{ij} = \overline{\rho u_i u_j}/\overline{\rho} = \widetilde{u_i u_j}$ are (Zeman, 1991)

$$1/2\frac{\partial q^2}{\partial t} = P_s - (\epsilon_s + \epsilon_d - \Pi_d), \tag{19}$$

$$\frac{\partial R_{12}}{\partial t} + C\frac{R_{12}}{\tau} = -0.4R_{22}S, \tag{20}$$

$$\frac{\partial R_{22}}{\partial t} + C\frac{R_{22}}{\tau} = 0.4P_s - \frac{C - 2(1 + (\epsilon_d - \Pi_d)/\epsilon_s)}{3}\epsilon_s, \tag{21}$$

$$\frac{\partial \epsilon_s}{\partial t} = -C_\epsilon\frac{(\epsilon_s - 0.75P_s)}{\tau}, \ \epsilon_d/\epsilon_s = F(M_t). \tag{22}$$

The above equations are based on the Z90 version of a compressible turbulence model. Here the return-to-isotropy constant is $C = 3.25$, $C_\epsilon = 3.7$, $\tau = q^2/\epsilon_s$, and $P_s = -R_{12}S$ is the rate of turbulence production by shear. The closure equations for the dilatation terms Π_d and ϵ_d are as outlined in Section 2.2.

As alluded to in Zeman and Blaisdell (1990) and shown in Figs 5 and 6, the model equations (11)-(14) possess two asymptotic solutions depending on the initial Mach number M_t. If M_t is identically zero, the solution agrees with the incompressible DNS and experimental data (Tavoularis 1985, Rogers *et al.* 1986). The kinetic energy and R_{ij} grow exponentially, i.e. $q^2 \propto R_{ij} \propto exp\{\lambda_o St\}$, and the turbulent time scale approaches a constant value dictated by the shear, i.e. $S\tau \approx 11.7$. If, on the other hand, M_t is initially finite, the model solutions asymptote to a new state characterized by $M_t = M_{t\infty} \approx 0.62$ and $S\tau \approx 7.3$. The energy growth is again exponential but with a smaller growth parameter $\lambda < \lambda_o$. Both the model and DNS data suggest that before the asymptotic state is reached, $\lambda = \lambda(M_t)$ decreases with increasing M_t, although the DNS data exhibit rather different transient behavior due likely to low DNS Reynolds numbers. The model-computed evolutions of M_t shown in Fig. 6 also include DNS data with the initial $M_{to} = 0.4$ (in order to match the initial behavior of the DNS-computed M_t, the model initial value of $S\tau$ was 3 rather than 5.9 used in the DNS computations). The general result of the asymptotic behavior is independent of the form of dilatation dissipation function. For example, using the relation $\epsilon_d/\epsilon_s \approx M_t^2$, the solutions approached almost the same asymptotic state as with the shocklet dissipation assumption. As evident from Fig. 6, the DNS data of M_t do not show any sign of converging toward an asymptote; however, this may be due to the lack of shock wave resolution.

3.3.1 Pressure-dilatation effects in shear turbulence.

The pressure-dilatation Π_d plays, in the shear-turbulence dynamics, an equally important role as ϵ_d, but its effect on turbulence is rather subtle. As turbulence approaches equilibrium (for $St > 5$), the average Π_d becomes a negative constant fraction of the local solenoidal dissipation. The model predicts $\Pi_d/\epsilon_s \approx -0.07$, while the DNS yields a somewhat smaller value (-0.05). The agreement between the DNS and model is surprisingly close considering the fact that in the model Π_d

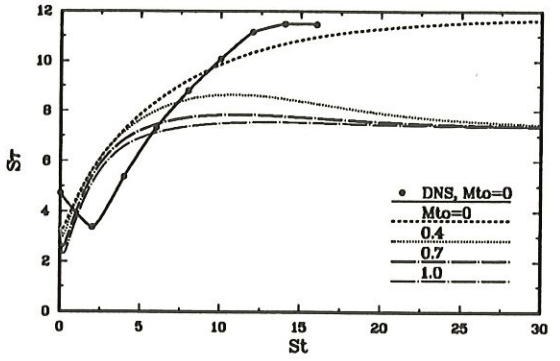

FIGURE 5. Evolution of turbulence time scale in shear turbulence.

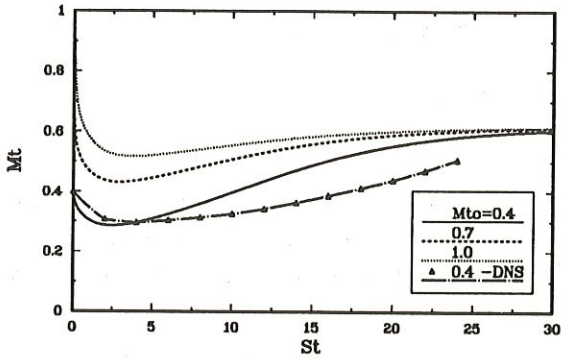

FIGURE 6. Evolution of r.m.s. Mach number M_t.

depends on the subtle difference between the current value of $\overline{p^2}$ and the equilibrium value p_e^2 in the pressure-relaxation model (17). Evidently, $\overline{p^2}$ always lags behind the equilibrium value which is continually growing with q^2 and M_t. Physically this means that as the kinetic energy is produced by shear, a fraction of it is transferred to the potential energy ($\propto \overline{p^2}$). The transfer is mediated by Π_d, and thus in the kinetic energy balance (19), $\Pi_d < 0$ represents a loss of the same order as ϵ_d.

The second, important aspect of the pressure-relaxation model is the capability to predict the pressure variance $\overline{p^2}$. This is demonstrated in Fig. 7, where $\overline{p^2}/\overline{\rho}^2$ is plotted vs. M_t; the cross-hatched area represents the spread of DNS data (Blaisdell, 1990), and full circles are the model results. The model-DNS agreement is satisfactory, and if necessary, further improvement could be made by adjusting the constant α in (18). It is noted that since the acoustic time scale τ_a is small compared with the time scale of evolution, it follows, according to (17), that $|\overline{p^2} - p_e^2|/\overline{\rho}^2 << 1$, and therefore, $\overline{p^2}/\overline{\rho}^2 \approx \gamma^2 M_t^2 P_e(M_t)$. The DNS data favor the M_t^2 -dependence in the equilibrium function P_e in (18).

In view of the above arguments and comparison with the DNS results, it is evident that the combined model for the pressure dilatation and pressure variance (in (17) and (18)) represents the essential physics of compressive-solenoidal field interactions

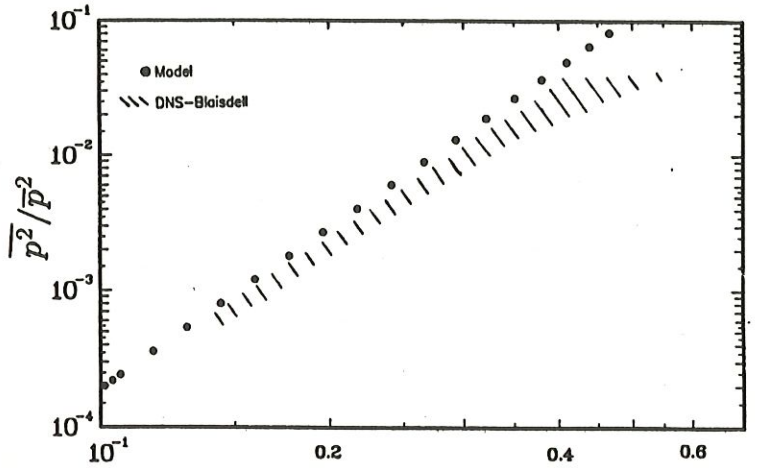

FIGURE 7. Normalized pressure variance in shear turbulence vs M_t.

in quasi-equilibrium shear turbulence.

4. Future plans

We plan to investigate the effect of mean compression (or expansion) on the structure of compressible decaying or shear-driven turbulence. In the presence of nonzero mean divergence $\nabla \cdot \mathbf{U}$, the pressure variance equation will contain a source term, i.e.,

$$\frac{1}{2}\frac{D\overline{p^2}}{Dt} = -(\overline{\rho}a)^2\Pi_d - \overline{p^2}\nabla \cdot \mathbf{U} + \textit{other terms}$$

This suggests that the pressure-dilatation term should have a form

$$\Pi_d = \frac{1}{2(\overline{\rho}a)^2}[\frac{\overline{p^2} - p_e^2}{\tau_a} + c_p\overline{p^2}\nabla \cdot \mathbf{U}] + ...$$

Hence, in analogy with the pressure-strain terms in incompressible turbulence, the first part of Π_d is the return-to-equilibrium term, and the second is a rapid term depending on the mean distortion $\nabla \cdot \mathbf{U}$. In the case of isotropic, homogeneous compression, the process of (rapid) compression can be treated by linear, rapid-distortion theory, and the unknown constant c_p associated with the rapid term in the Π_d-model above can be determined.

The future work will focus on the inhomogeneous rapid compression taking place when turbulence passes through a shock or a succession of shocks. Preliminary results indicate that one-dimensional compression has considerable influence on the structural parameters of shear-maintained turbulence.

REFERENCES

BLAISDELL, G. A. 1990 Numerical simulations of compressible homogeneous turbulence. *Ph. D. Thesis.* Mechanical Engineering Dept., Stanford University.

CHANDRASEKHAR, S. 1952 The fluctuations of density in isotropic turbulence. *Proc. Roy. Soc. A.* **210**, 18.

KOVÁSZNAY, L. S. G. 1953 Turbulence in supersonic flow. *J. Aeronaut. Sci.* **20**, 657.

LEE, S., LELE, S., & MOIN, P. 1990 Eddy-shocklets in decaying compressible turbulence. CTR Report No. 110, Stanford University (to be published in *Phys. Fluids*).

PAPAMOSCHOU, D., & ROSHKO, A. 1988 The compressible turbulent shear layer: an experimental study. *J. Fluid Mech.* **197**, 453.

ROGERS, M. M., MOIN, P., & REYNOLDS, W. C. 1986 Report No. TF-25, Stanford University.

SAMIMY, M. & ELLIOTT, G. S. 1990 The effects of compressibility on the characteristics of free shear layers. *AIAA J.* **28**, 429.

TAVOULARIS, S. 1985 Asymptotic laws for transversely homogeneous turbulent shear flows. *Phys. Fluids.* **28**, 999.

ZEMAN, O. 1990a Dilatation dissipation: The concept and application in modeling compressible mixing layers. *Phys. Fluids A.* **2**, 178.

ZEMAN, O. 1990b Similarity in supersonic mixing layers. submitted to *AIAA J.*

ZEMAN, O. 1990c On the decay of compressible isotropic turbulence. CTR Report No. 115, Stanford University (submitted to *Phys. Fluids*).

ZEMAN, O., & BLAISDELL, G. A. 1990 New physics and models for compressible turbulence. In *Advances of Turbulence 3.* Springer-Verlag.

ZEMAN, O. 1991 Toward a constitutive relation in compressible turbulence. Proceedings of the Lumley's 60th Birthday Symposium.